

## Recombinant methioninase combined with doxorubicin (DOX) regresses a DOX-resistant synovial sarcoma in a patient-derived orthotopic xenograft (PDOX) mouse model

Kentaro Igarashi<sup>1,2,3</sup>, Kei Kawaguchi<sup>1,2</sup>, Shukuan Li<sup>1</sup>, Qinghong Han<sup>1</sup>, Yuying Tan<sup>1</sup>, Emily Gainor<sup>1</sup>, Tasuku Kiyuna<sup>1,2</sup>, Kentaro Miyake<sup>1,2</sup>, Masuyo Miyake<sup>1,2</sup>, Takashi Higuchi<sup>1,2</sup>, Hiromichi Oshiro<sup>1,2</sup>, Arun S. Singh<sup>4</sup>, Mark A. Eckardt<sup>5</sup>, Scott D. Nelson<sup>6</sup>, Tara A. Russell<sup>7</sup>, Sarah M. Dry<sup>6</sup>, Yunfeng Li<sup>6</sup>, Norio Yamamoto<sup>3</sup>, Katsuhiko Hayashi<sup>3</sup>, Hiroaki Kimura<sup>3</sup>, Shinji Miwa<sup>3</sup>, Hiroyuki Tsuchiya<sup>3</sup>, Fritz C. Eilber<sup>7</sup> and Robert M. Hoffman<sup>1,2</sup>

<sup>1</sup>AntiCancer, Inc., San Diego, California, USA

<sup>2</sup>Department of Surgery, University of California, San Diego, California, USA

<sup>3</sup>Department of Orthopaedic Surgery, Kanazawa University, Kanazawa, Japan

<sup>4</sup>Division of Hematology-Oncology, University of California, Los Angeles, CA, USA

<sup>5</sup>Department of Surgery, Yale School of Medicine, New Haven, Connecticut, USA

<sup>6</sup>Department of Pathology, University of California, Los Angeles, CA, USA

<sup>7</sup>Division of Surgical Oncology, University of California, Los Angeles, CA, USA

**Correspondence to:** Robert M. Hoffman, **email:** all@anticancer.com

Fritz C. Eilber, **email:** fceilber@mednet.ucla.edu

Hiroyuki Tsuchiya, **email:** tsuchi@med.kanazawa-u.ac.jp

**Keywords:** synovial sarcoma; patient-derived orthotopic xenograft; PDOX; recombinant methioninase; doxorubicin

**Received:** February 22, 2018

**Accepted:** March 15, 2018

**Published:** April 10, 2018

**Copyright:** Igarashi et al. This is an open-access article distributed under the terms of the Creative Commons Attribution License 3.0 (CC BY 3.0), which permits unrestricted use, distribution, and reproduction in any medium, provided the original author and source are credited.

### ABSTRACT

**Synovial sarcoma (SS) is a recalcitrant subgroup of soft tissue sarcoma (STS). A tumor from a patient with high grade SS from a lower extremity was grown orthotopically in the right biceps femoris muscle of nude mice to establish a patient-derived orthotopic xenograft (PDOX) mouse model. The PDOX mice were randomized into the following groups when tumor volume reached approximately 100 mm<sup>3</sup>: G1, control without treatment; G2, doxorubicin (DOX) (3 mg/kg, intraperitoneal [i.p.] injection, weekly, for 2 weeks; G3, rMETase (100 unit/mouse, i.p., daily, for 2 weeks); G4 DOX (3mg/kg), i.p. weekly, for 2 weeks) combined with rMETase (100 unit/mouse, i.p., daily, for 2 weeks). On day 14 after treatment initiation, all therapies significantly inhibited tumor growth compared to untreated control, except DOX: (DOX:  $p = 0.48$ ; rMETase:  $p < 0.005$ ; DOX combined with rMETase  $< 0.0001$ ). DOX combined with rMETase was significantly more effective than both DOX alone ( $p < 0.001$ ) and rMETase alone ( $p < 0.05$ ). The relative body weight on day 14 compared with day 0 did not significantly differ between any treatment group or untreated control. The results indicate that r-METase can overcome DOX-resistance in this recalcitrant disease.**

### INTRODUCTION

Sarcoma is a group of 50 or more rare recalcitrant cancers [1]. In order to improve the outcome of sarcoma patients, we have developed patient-derived orthotopic xenograft (PDOX) models of the major sarcomas: soft-

tissue sarcoma [2–4], follicular dendritic-cell sarcoma [5], Ewing's sarcoma [6–10], undifferentiated pleomorphic soft-tissue sarcoma [11, 12], osteosarcoma [13–16, 25], rhabdomyosarcoma [17, 18], leiomyosarcoma [19] and undifferentiated spindle-cell sarcoma (USCS) [20, 23, 26]. During the course of finding more efficacious

agents for this group of diseases, we have found that our developmental therapeutic, recombinant methioninase (rMETase), is active and can inhibit or arrest tumor growth and in combination with an appropriate chemotherapy drug, can regress the PDOX tumors [7, 21–26].

rMETase effectively reduced tumor growth of a DOX-resistant *FUS-ERG* Ewing's sarcoma PDOX [6] compared to untreated control. The methionine level both of plasma and supernatants derived from sonicated tumors was lower in the rMETase group [7].

An undifferentiated spindle-cell sarcoma (USCS) PDOX model was treated with rMETase. rMETase inhibited tumor growth, measured by tumor volume, compared to untreated controls and first-line therapy doxorubicin (DOX). Tumor L-methionine levels were reduced after rMETase-treatment [26].

In a subsequent study, we determined the efficacy of rMETase in combination with DOX in a PDOX model of USCS. rMETase in combination with DOX could regress the USCS PDOX model [23].

Synovial sarcoma (SS) is an aggressive subtype that accounts for 10% to 20% of soft tissue sarcoma (STS) in the adolescent and young adult population [27]. Treatment for localized SS consists of a combination of surgery, radiotherapy and, in some cases, chemotherapy. Chemotherapy has a low response rate for metastatic disease [28]. Treatment is usually wide surgical excision with adjuvant or neoadjuvant therapy. In the present study, we determined if rMETase could overcome first-line DOX-resistance in a PDOX model of SS.

## RESULTS AND DISCUSSION

On day 14 after initiation, DOX ( $p = 0.48$ ) was ineffective on the SS PDOX. rMETase ( $p < 0.005$ ) inhibited tumor growth and DOX combined with rMETase ( $p < 0.0001$ ) regressed tumor growth. DOX combined with rMETase was significantly more effective than both DOX alone ( $p < 0.001$ ) and rMETase alone ( $p < 0.05$ ) (Figures 1–3). The relative body weight on day 14 compared with day 0 did not significantly differ between any treatment group (Figure 4).

### Histology

High-power photomicrographs of hematoxylin and eosin (H&E)-stained sections of the original patient tumor showed cancer cells with hyperchromatic, enlarged nuclei. Mitotic figures and atypical cells are present (Figure 5A). A high-power view of the untreated SS PDOX model showed similar features, including cells with hyperchromatic and enlarged nuclei. Mitotic figures, including atypical forms, are also present (Figure 5B). Tumors treated with DOX comprised viable cells without apparent necrosis or inflammatory changes (Figure 5C). Tumors treated with rMETase show altered cancer-cell shape and some necrosis (Figure 5D). Tumors treated with

DOX combined with rMETase have extensive necrosis (Figure 5E).

There was a statistically-significant difference in tumor growth between either the untreated control or the DOX-treated PDOX, on the one hand, and either the rMETase- or the combination of rMETase and DOX-treated PDOX on the other. There was also a statistically-significant difference between the rMETase-treated and the combination rMETase-treated and DOX-treated PDOX. During the treatment period, there was no body-weight loss in any treated group.

Methionine restriction of cancer results in an S/G<sub>2</sub>-phase cell-cycle arrest that eventually leads to cancer-cell death [29–31]. This is the probable mechanism for necrosis in the rMETase-treated PDOX which is further exacerbated by the addition of DOX to rMETase.

Lung metastasis in the synovial sarcoma and its sensitivity to rMETase will be a topic for future study.

Our laboratory has developed PDOX mouse models of cancer for discovery of transformative therapy for recalcitrant cancer. The PDOX nude mouse model is established with the technique of surgical orthotopic implantation (SOI). These models include breast [32], ovarian [33], lung [34], cervical [35], colon [36–38], pancreatic [39–43] and stomach cancer [44], melanoma [21, 22, 24, 45–48] as well as sarcoma [2–20, 23, 25, 26]. The PDOX model, developed by our laboratory over the past 30 years, has many advantages over subcutaneous-transplant models which grow ectopically under the skin and rarely can metastasize [49].

We have recently demonstrated that rMETase is effective against a PDOX model of Ewing's sarcoma [7]. We have also found rMETase to be effective in a PDOX model of DOX-resistant spindle cell sarcoma [26] and to overcome DOX-resistance in the spindle-cell sarcoma PDOX [23].

All PDOX models tested thus far, including those derived from Ewing's sarcoma [7], osteosarcoma [15], spindle-cell sarcoma [23, 26], and melanoma [21, 22, 24] are very sensitive to rMETase, and in combination with first-line chemotherapy, rMETase can regress PDOX tumors. These results, in addition to extensive *in vitro* and *in vivo* cell line studies showing MET-dependence and response to rMETase or other means of MET-restriction [29, 30, 50–55] suggest rMETase is a general therapeutic for all cancer. Extensive safety tests were performed with rMETase in primates [56, 57] and initial testing in humans [58, 59] indicated minimal toxicity of rMETase. Very recently we have shown that rMETase can be administered orally [24], suggesting the near-future widespread use of rMETase for all types of cancer in the clinic.

Methionine dependence is due to the overuse of methionine for aberrant transmethylation reactions in cancer and is possibly the only known general metabolic defect in cancer [50, 60–66].

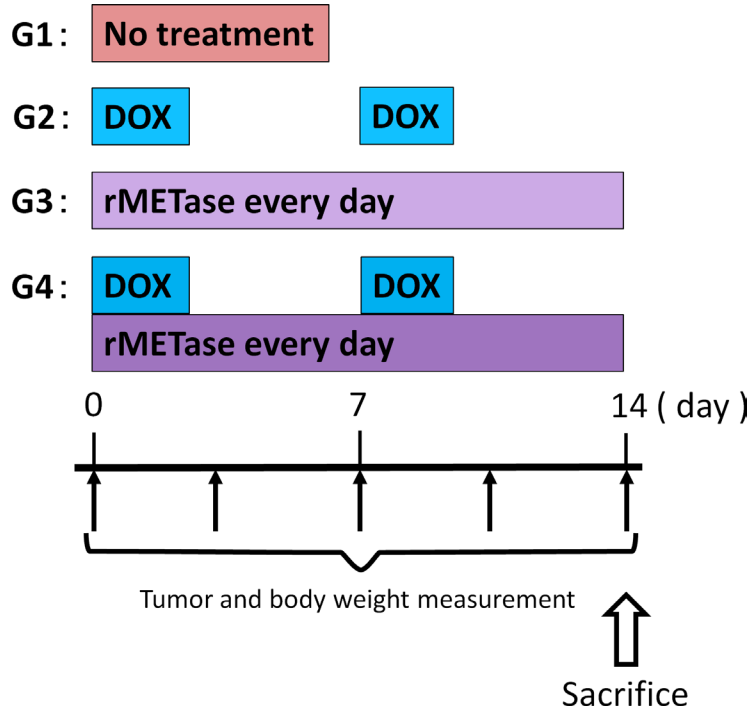


Figure 1: Treatment schema.

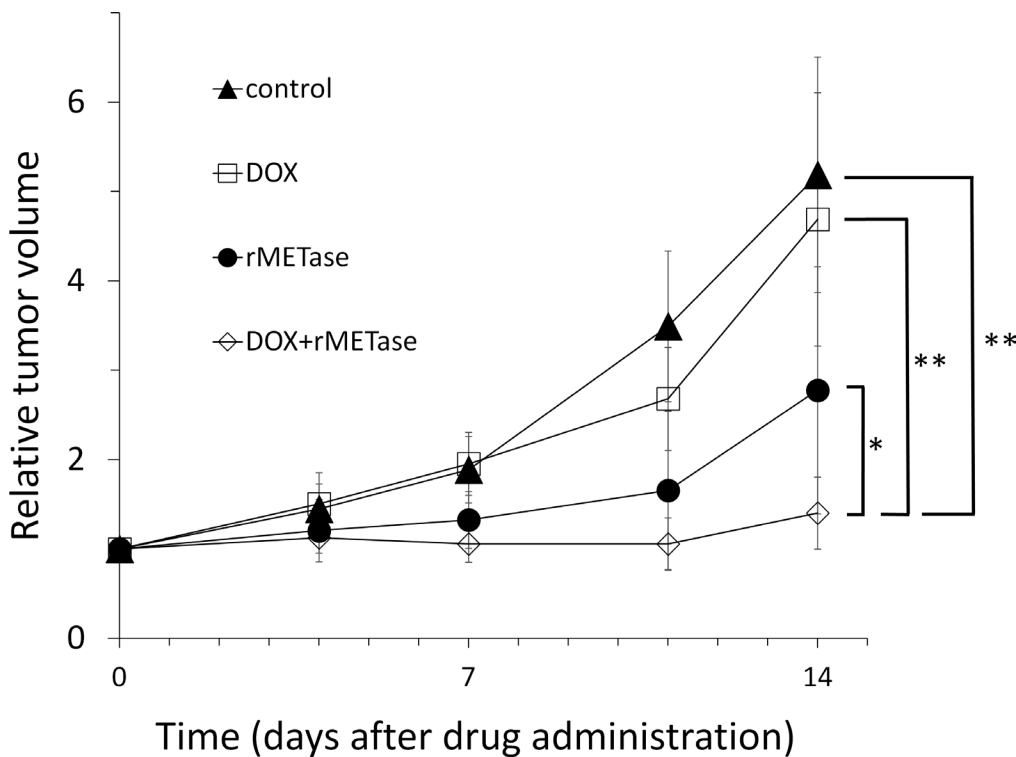


Figure 2: *In vivo* antitumor efficacy of doxorubicin (DOX), l-methionine  $\alpha$ -deamino- $\gamma$ -mercaptomethane lyase (rMETase) and DOX combined with rMETase. Synovial sarcoma was grown orthotopically in the right biceps femoris muscle of nude mice and allowed to form tumors. Treatment, dose, route, and schedule were: DOX (3 mg/kg/week i.p. for 2 weeks), and rMETase (100 U/mouse/day, i.p., for 14 days). Relative tumor volume, shown by the line graphs, is the tumor volume at the indicated time points during the time of treatment divided by the tumor volume at the onset of treatment.  $N = 8$  mice/group. \* $p < 0.05$ , \*\* $p < 0.001$ .

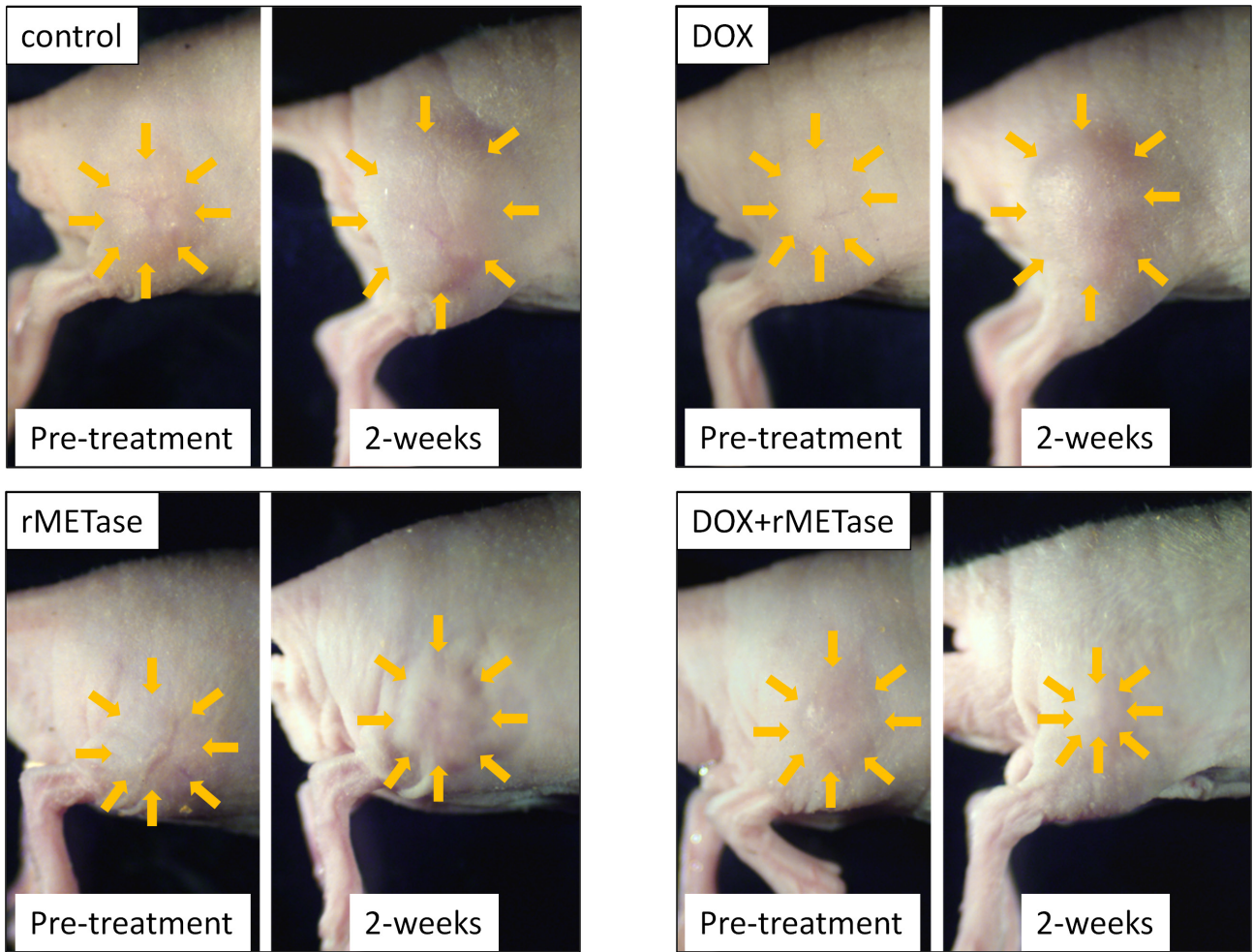


Figure 3: Photos of representative treated and untreated SS PDOX tumor.

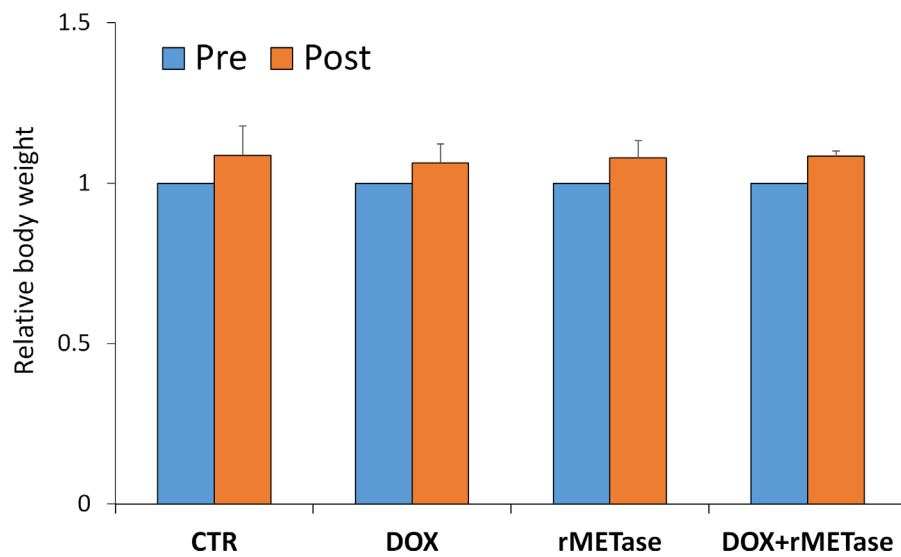
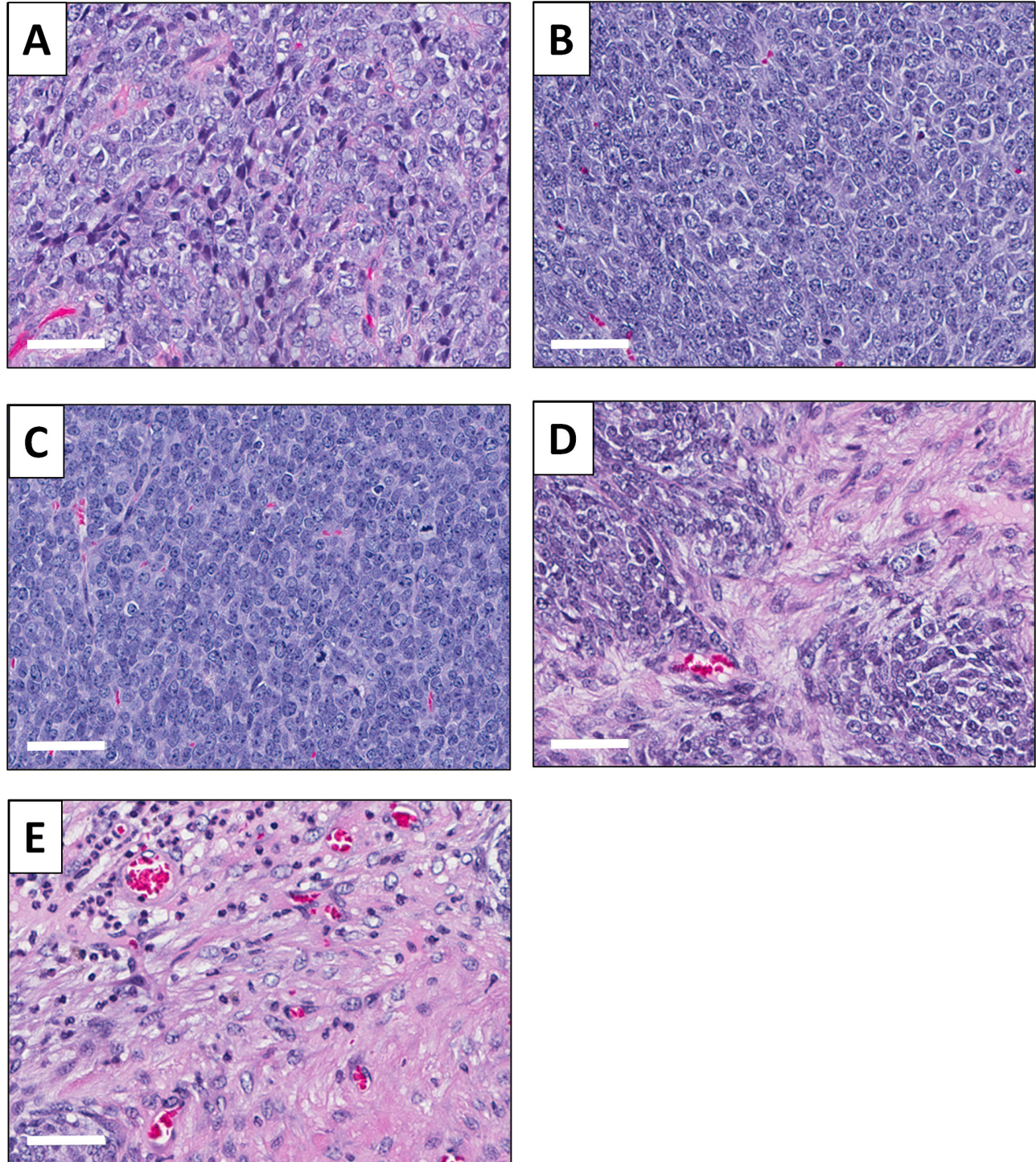


Figure 4: Bar graph shows body weight in each group at pre-treatment and 2 weeks after drug administration. There were no significant differences between any group.

The overuse of methionine by cancer cells for enhanced and unbalanced transmethylation may be the basis of the methionine dependence of cancer cells and is termed the “Hoffman effect”, analogous to the Warburg effect of glucose overuse in cancer [64]. The

Hoffman effect can be observed clinically in [<sup>11</sup>C]MET PET imaging which gives a much stronger signal than fluorodeoxyglucose (FDG)-PET [67].

Previously-developed concepts and strategies of highly-selective tumor targeting can take advantage of



**Figure 5: Tumor histology.** (A) H&E-stained section of the original SS patient tumor; (B) untreated SS PDOX tumor; (C) SS PDOX tumor treated with DOX; (D) SS PDOX tumor treated with rMETase and (E) SS PDOX tumor treated with DOX combined with rMETase. White scale bars: 50  $\mu$ m.

molecular targeting of tumors, including tissue-selective therapy which focuses on unique differences between normal and tumor tissues [68–73].

## MATERIALS AND METHODS

### Mice

Athymic *nu/nu* male nude mice (AntiCancer, Inc., San Diego, CA), 4–6 weeks old, were used in this study. All mice were kept in a barrier facility on a high efficiency particulate arrestance (HEPA)-filtered rack under standard conditions of 12-hour light/dark cycles. The animals were fed an autoclaved laboratory rodent diet. All animal experiments were performed with an AntiCancer Institutional Animal Care and Use Committee (IACUC)-protocol specifically approved for this study and in accordance with the principals and procedures outlined in the National Institutes of Health Guide for the Care and Use of Animals under Assurance Number A3873-1. Anesthesia and analgesics were used for all surgical experiments to avoid excessive suffering of the mice. A ketamine mixture (0.02 ml solution of 20 mg/kg ketamine, 15.2 mg/kg xylazine, and 0.48 mg/kg acepromazine maleate) was used subcutaneously for all mice. The animals were monitored carefully during surgery to keep adequate depth of anesthesia. The animals were observed daily and humanely sacrificed by CO<sub>2</sub> inhalation when they met the following criteria: severe tumor burden (more than 20 mm in diameter), prostration, significant body weight loss, difficulty breathing, rotational motion and body temperature drop.

### Patient-derived tumor

A 45-year-old male diagnosed with primary synovial sarcoma on the lower leg underwent surgical resection at the Department of Surgery, University of California, Los Angeles (UCLA). Written informed consent was obtained from the patient as part of a UCLA Institutional Review Board (IRB #10-001857)-approved protocol. The patient received neo-adjuvant doxorubicin-based chemotherapy prior to surgery.

### Surgical orthotopic implantation (SOI) for establishment of PDOX model

A fresh sample of the tumor of the patient was obtained and transported immediately to the laboratory at AntiCancer, Inc., on wet ice. The sample was cut into 5 mm fragments and initially implanted subcutaneously in nude mice. The grown tumors were cut into small fragments (3–4 mm). After nude mice were anesthetized, a 5 mm skin incision was made on the right high thigh, and biceps femoris was split to make space for the tumor. A single tumor fragment was implanted orthotopically

into the space to establish a PDOX model. The wound was closed with 6-0 nylon suture (Ethilon, Ethicon, Inc., NJ, USA).

### rMETase production

The pAC-1 rMETase high-expression clone was used for rMETase production. The fermentation procedure for host *E.coli* cells and the purification protocol for rMETase were the same as previously described: rMETase was purified by 3 different steps using columns of DEAE Sepharose FF, Sephacryl S-200HR, and ActiClean Etox, which is designed for eliminating endotoxin [74].

### Treatment study design in the PDOX model of synovial sarcoma

SS PDOX mouse models were randomized into 4 groups of 8 mice each: G1, control without treatment; G2, Doxorubicin (DOX) (3 mg/kg, intraperitoneal [i.p.] injection, weekly, for 2 weeks); G3, rMETase (100 unit/mouse, i.p., daily, for 2 weeks); G4, DOX (3 mg/kg), i.p. weekly, for 2 weeks) combined with rMETase (100 unit/mouse, i.p., daily, for 2 weeks) (Figure 1). Tumor length, width and mouse body weight were measured twice in a week. Tumor volume was calculated with the following formula: Tumor volume (mm<sup>3</sup>) = length (mm) × width (mm) × width (mm) × 1/2. Data are presented as mean ± SD.

### Histological examination

Fresh tumor samples were fixed in 10% formalin and embedded in paraffin before sectioning and staining. Tissue sections (3 μm) were deparaffinized in xylene and rehydrated in an ethanol series. Hematoxylin and eosin (H&E) staining was performed according to standard protocol. Histological examination was performed with a BHS system microscope. Images were acquired with INFINITY ANALYZE software (Lumenera Corporation, Ottawa, Canada).

## CONFLICTS OF INTEREST

None.

## REFERENCES

1. Clark MA, Fisher C, Judson I, Thomas JM. Soft-tissue sarcomas in adults. *N Engl J Med*. 2005; 353:701–711.
2. Hiroshima Y, Zhang Y, Zhang N, Uehara F, Maawy A, Murakami T, Mii S, Yamamoto M, Miwa S, Yano S, Momiyama M, Mori R, Matsuyama R, et al. Patient-derived orthotopic xenograft (PDOX) nude mouse model of soft-tissue sarcoma more closely mimics the patient behavior in contrast to the subcutaneous ectopic model. *Anticancer Res*. 2015; 35:697–701.

3. Hiroshima Y, Zhao M, Zhang Y, Zhang N, Maawy A, Murakami T, Mii S, Uehara F, Yamamoto M, Miwa S, Yano S, Momiyama M, Mori R, et al. Tumor-targeting *Salmonella typhimurium* A1-R arrests a chemo-resistant patient soft-tissue sarcoma in nude mice. *PLoS One*. 2015; 10:e0134324.
4. Murakami T, DeLong J, Eilber FC, Zhao M, Zhang Y, Zhang N, Singh A, Russell T, Deng S, Reynoso J, Quan C, Hiroshima Y, Matsuyama R, et al. Tumor-targeting *Salmonella typhimurium* A1-R in combination with doxorubicin eradicate soft tissue sarcoma in a patient-derived orthotopic xenograft PDOX model. *Oncotarget*. 2016; 7:12783–12790. <https://doi.org/10.18632/oncotarget.7226>.
5. Kiyuna T, Murakami T, Tome Y, Kawaguchi K, Igarashi K, Zhang Y, Zhao M, Li Y, Bouvet M, Kanaya F, Singh A, Dry S, Eilber FC, et al. High efficacy of tumor-targeting *Salmonella typhimurium* A1-R on a doxorubicin- and dactolisib-resistant follicular dendritic-cell sarcoma in a patient-derived orthotopic xenograft PDOX nude mouse model. *Oncotarget*. 2016; 7:33046–33054. <https://doi.org/10.18632/oncotarget.8848>.
6. Murakami T, Singh AS, Kiyuna T, Dry SM, Li Y, James AW, Igarashi K, Kawaguchi K, DeLong JC, Zhang Y, Hiroshima Y, Russell T, Eckardt MA, et al. Effective molecular targeting of CDK4/6 and IGF-1R in a rare FUS-ERG fusion CDKN2A-deletion doxorubicin-resistant Ewing's sarcoma in a patient-derived orthotopic xenograft (PDOX) nude-mouse model. *Oncotarget*. 2016; 7:47556–47564. <https://doi.org/10.18632/oncotarget.9879>.
7. Murakami T, Li S, Han Q, Tan Y, Kiyuna T, Igarashi K, Kawaguchi K, Hwang HK, Miyaki K, Singh AS, Hiroshima Y, Lwin TM, DeLong JC, et al. Recombinant methioninase effectively targets a Ewing's sarcoma in a patient-derived orthotopic xenograft (PDOX) nude-mouse model. *Oncotarget*. 2017; 8:35630–35638. <https://doi.org/10.18632/oncotarget.15823>.
8. Murakami T, Kiyuna T, Kawaguchi K, Igarashi K, Singh AS, Hiroshima Y, Zhang Y, Zhao M, Miyake K, Nelson SD, Dry SM, Li Y, DeLong JC, et al. The irony of highly-effective bacterial therapy of a patient-derived orthotopic xenograft (PDOX) model of Ewing's sarcoma, which was blocked by Ewing himself 80 years ago. *Cell Cycle*. 2017; 16:1046–1052.
9. Miyake K, Murakami T, Kiyuna T, Igarashi K, Kawaguchi K, Miyake M, Li Y, Nelson SD, Dry SM, Bouvet M, Elliott IA, Russell TA, Singh AS, et al. The combination of temozolomide-irinotecan regresses a doxorubicin-resistant patient-derived orthotopic xenograft (PDOX) nude-mouse model of recurrent Ewing's sarcoma with a FUS-ERG fusion and CDKN2A deletion: Direction for third-line patient therapy. *Oncotarget*. 2017; 8:103129–103136. <https://doi.org/10.18632/oncotarget.20789>.
10. Miyake K, Murakami T, Kiyuna T, Igarashi K, Kawaguchi K, Li Y, Singh AS, Dry SM, Eckardt MA, Hiroshima Y, Momiyama M, Matsuyama R, Chishima T, et al. Eribulin regresses a doxorubicin-resistant Ewing's sarcoma with a FUS-ERG fusion and CDKN2A-deletion for the patient-derived orthotopic xenograft (PDOX) nude mouse model. *J Cell Biochem*. 2018; 119:967–972.
11. Kiyuna T, Murakami T, Tome Y, Igarashi K, Kawaguchi K, Russell T, Eckhardt MA, Crompton J, Singh A, Bernthal N, Bukata S, Federman N, Kanaya F, et al. Labeling the stroma of a patient-derived orthotopic xenograft (PDOX) mouse models of undifferentiated pleomorphic soft-tissue sarcoma with red fluorescent protein for rapid non-invasive drug screening. *J Cell Biochem*. 2017; 118:361–365.
12. Igarashi K, Kawaguchi K, Murakami T, Kiyuna T, Miyake K, Yamamoto N, Hayashi K, Kimura H, Nelson SD, Dry SM, Li Y, Singh A, Miwa S, et al. A novel anionic-phosphate-platinum complex effectively targets an undifferentiated pleomorphic sarcoma better than cisplatin and doxorubicin in a patient-derived orthotopic xenograft (PDOX). *Oncotarget*. 2017; 8:63353–63359. <https://doi.org/10.18632/oncotarget.18806>.
13. Murakami T, Igarashi K, Kawaguchi K, Kiyuna T, Zhang Y, Zhao M, Hiroshima Y, Nelson SD, Dry SM, Li Y, Yanagawa J, Russell T, Federman N, et al. Tumor-targeting *Salmonella typhimurium* A1-R regresses an osteosarcoma in a patient-derived xenograft model resistant to a molecular-targeting drug. *Oncotarget*. 2017; 8:8035–8042. <https://doi.org/10.18632/oncotarget.14040>.
14. Igarashi K, Kawaguchi K, Murakami T, Kiyuna T, Miyake K, Nelson SD, Dry SM, Li Y, Yanagawa J, Russell TA, Singh A, Yamamoto N, Hayashi K, et al. Intra-arterial administration of tumor-targeting *Salmonella typhimurium* A1-R regresses a cisplatin-resistant relapsed osteosarcoma in a patient-derived orthotopic xenograft (PDOX) mouse model. *Cell Cycle*. 2017; 16:1164–1170.
15. Igarashi K, Murakami T, Kawaguchi K, Kiyuna T, Miyake K, Zhang Y, Nelson SD, Dry SM, Li Y, Yanagawa J, Russell TA, Singh AS, Tsuchiya H, et al. A patient-derived orthotopic xenograft (PDOX) mouse model of an cisplatin-resistant osteosarcoma lung metastasis that was sensitive to temozolomide and trabectedin: implications for precision oncology. *Oncotarget*. 2017; 8:62111–62119. <https://doi.org/10.18632/oncotarget.19095>.
16. Igarashi K, Kawaguchi K, Kiyuna T, Miyake K, Miyake M, Li Y, Nelson SD, Dry SM, Singh AS, Elliott I, Russell TA, Eckhardt MA, Yamamoto N, et al. Temozolomide combined with irinotecan regresses a cisplatin-resistant relapsed osteosarcoma in a patient-derived orthotopic xenograft (PDOX) precision-oncology mouse model. *Oncotarget*. 2018; 9:7774–7781. <https://doi.org/10.18632/oncotarget.22892>.
17. Igarashi K, Kawaguchi K, Kiyuna T, Murakami T, Miwa S, Nelson SD, Dry SM, Li Y, Singh A, Kimura H, Hayashi

- K, Yamamoto N, Tsuchiya H, et al. Patient-derived orthotopic xenograft (PDOX) mouse model of adult rhabdomyosarcoma invades and recurs after resection in contrast to the subcutaneous ectopic model. *Cell Cycle*. 2017; 16:91–94.
18. Igarashi K, Kawaguchi K, Kiyuna T, Murakami T, Miwa S, Nelson SD, Dry SM, Li Y, Singh A, Kimura H, Hayashi K, Yamamoto N, Tsuchiya H, et al. Temozolomide combined with irinotecan caused regression in an adult pleomorphic rhabdomyosarcoma patient-derived orthotopic xenograft (PDOX) nude-mouse model. *Oncotarget*. 2017; 8:75874–75880. <https://doi.org/10.18632/oncotarget.16548>.
  19. Kawaguchi K, Igarashi K, Murakami T, Kiyuna T, Nelson SD, Dry SM, Li Y, Russell TA, Singh AS, Chmielowski B, Unno M, Eilber FC, Hoffman RM. Combination of gemcitabine and docetaxel regresses both gastric leiomyosarcoma proliferation and invasion in an imageable patient-derived orthotopic xenograft (iPDOX) model. *Cell Cycle*. 2017; 16:1063–1069.
  20. Igarashi K, Kawaguchi K, Murakami T, Kiyuna T, Miyake K, Singh A, Nelson SD, Dry SM, Li Y, Yamamoto N, Hayashi K, Kimura H, Miwa S, et al. High efficacy of pazopanib on an undifferentiated spindle-cell sarcoma resistant to first-line therapy is identified with a patient-derived orthotopic xenograft (PDOX) nude mouse model. *J Cell Biochem*. 2017; 118:2739–3743.
  21. Kawaguchi K, Igarashi K, Li S, Han Q, Tan Y, Kiyuna T, Miyake Y, Murakami T, Chmielowski B, Nelson SD, Russell TA, Dry SM, Li Y, et al. Combination treatment with recombinant methioninase enables temozolomide to arrest a BRAF V600E melanoma growth in a patient-derived orthotopic xenograft. *Oncotarget*. 2017; 8:85516–85525. <https://doi.org/10.18632/oncotarget.20231>.
  22. Kawaguchi K, Igarashi K, Li S, Han Q, Tan Y, Miyake K, Kiyuna T, Miyake M, Murakami T, Chmielowski S, Nelson SD, Russell TA, Dry SM, et al. Recombinant methioninase (rMETase) is an effective therapeutic for BRAF-V600E-negative as well as -positive melanoma in patient-derived orthotopic xenograft (PDOX) mouse models. *Oncotarget*. 2019; 9:915–923. <https://doi.org/10.18632/oncotarget.23185>.
  23. Igarashi K, Kawaguchi K, Li S, Han Q, Tan Y, Murakami T, Kiyuna T, Miyake K, Miyake M, Singh AS, Eckhardt MA, Nelson SD, Russell TA, et al. Recombinant methioninase in combination with DOX overcomes first-line DOX resistance in a patient-derived orthotopic xenograft nude-mouse model of undifferentiated spindle-cell sarcoma. *Cancer Letters*. 2018; 417:168–173.
  24. Kawaguchi K, Han Q, Li S, Tan Y, Igarashi K, Kiyuna T, Miyake K, Miyake M, Chmielowski B, Nelson SD, Russell TA, Dry SM, Li Y, et al. Targeting methionine with oral recombinant methioninase (o-rMETase) arrests a patient-derived orthotopic xenograft (PDOX) model of BRAF-V600E mutant melanoma: implications for clinical cancer therapy and prevention. *Cell Cycle*. 2018 Mar 19:1–6. [Epub ahead of print].
  25. Igarashi K, Kawaguchi K, Kiyuna T, Miyake K, Miyake M, Li S, Han Q, Tan Y, Zhao M, Li Y, Nelson SD, Dry SM, Singh AS, et al. Tumor-targeting Salmonella typhimurium A1-R combined with recombinant methioninase and cisplatin eradicates an osteosarcoma cisplatin-resistant lung metastasis in a patient-derived orthotopic xenograft (PDOX) mouse model: Decoy, trap and kill chemotherapy moves toward the clinic. *Cell Cycle*. 2018 Jan 29:1–31. [Epub ahead of print].
  26. Igarashi K, Li S, Han Q, Tan Y, Kawaguchi K, Murakami T, Kiyuna T, Miyake K, Li Y, Nelson SD, Dry SM, Singh AS, Elliott I, et al. Growth of a doxorubicin-resistant undifferentiated spindle-cell sarcoma PDOX is arrested by metabolic targeting with recombinant methioninase. *J Cell Biochem*. 2018; 119:3537–3544.
  27. Herzog CE. Overview of sarcomas in the adolescent and young adult population. *J Pediatr Hematol Oncol*. 2005; 27:215–218.
  28. Eilber FC, Brennan MF, Eilber FR, Eckardt JJ, Grobmyer SR, Riedel E, Forscher C, Maki RG, Singer S. Chemotherapy is associated with improved survival in adult patients with primary extremity synovial sarcoma. *Ann Surg*. 2007; 246:105–113.
  29. Yano S, Takehara K, Zhao M, Tan Y, Han Q, Li S, Bouvet M, Fujiwara T, Hoffman RM. Tumor-specific cell-cycle decoy by Salmonella typhimurium A1-R combined with tumor-selective cell-cycle trap by methioninase overcome tumor intrinsic chemoresistance as visualized by FUCCI imaging. *Cell Cycle*. 2016; 15:1715–1723.
  30. Yano S, Li S, Han Q, Tan Y, Bouvet M, Fujiwara T, Hoffman RM. Selective methioninase-induced trap of cancer cells in S/G2 phase visualized by FUCCI imaging confers chemosensitivity. *Oncotarget*. 2014; 5:8729–8736. <https://doi.org/10.18632/oncotarget.2369>.
  31. Hoffman RM, Jacobsen SJ. Reversible growth arrest in simian virus 40-transformed human fibroblasts. *Proc Natl Acad Sci USA*. 1980; 77:7306–7310.
  32. Fu X, Le P, Hoffman RM. A metastatic-orthotopic transplant nude-mouse model of human patient breast cancer. *Anticancer Res*. 1993; 13:901–904.
  33. Fu X, Hoffman RM. Human ovarian carcinoma metastatic models constructed in nude mice by orthotopic transplantation of histologically-intact patient specimens. *Anticancer Res*. 1993; 13:283–286.
  34. Wang X, Fu X, Hoffman RM. A new patient-like metastatic model of human lung cancer constructed orthotopically with intact tissue via thoracotomy in immunodeficient mice. *Int J Cancer*. 1992; 51:992–995.
  35. Hiroshima Y, Zhang Y, Zhang N, Maawy A, Mii S, Yamamoto M, Uehara F, Miwa S, Yano S, Murakami T, Momiyama M, Chishima T, Tanaka K, et al. Establishment

- of a patient-derived orthotopic xenograph (PDOX) model of HER-2-positive cervical cancer expressing the clinical metastatic pattern. *PLoS One*. 2015; 10:e0117417.
36. Fu X, Besterman JM, Monosov A, Hoffman RM. Models of human metastatic colon cancer in nude mice orthotopically constructed by using histologically intact patient specimens. *Proc Natl Acad Sci USA*. 1991; 88:9345–9349.
  37. Metildi CA, Kaushal S, Luiken GA, Talamini MA, Hoffman RM, Bouvet M. Fluorescently-labeled chimeric anti-CEA antibody improves detection and resection of human colon cancer in a patient-derived orthotopic xenograft (PDOX) nude mouse model. *J Surg Oncol*. 2014; 109:451–458.
  38. Hiroshima Y, Maawy A, Metildi CA, Zhang Y, Uehara F, Miwa S, Yano S, Sato S, Murakami T, Momiyama M, Chishima T, Tanaka K, Bouvet M, et al. Successful fluorescence-guided surgery on human colon cancer patient-derived orthotopic xenograft mouse models using a fluorophore-conjugated anti-CEA antibody and a portable imaging system. *J Laparoendosc Adv Surg Tech A*. 2014; 24:241–247.
  39. Kawaguchi K, Han Q, Li S, Tan Y, Igarashi K, Miyake K, Kiyuna T, Miyake M, Chmielowski B, Nelson SD, Russell TA, Dry SM, Li Y, et al. Intra-tumor L-methionine level highly correlates with tumor size in both pancreatic cancer and melanoma patient-derived orthotopic xenograft (PDOX) nude-mouse models. *Oncotarget*. 2018; 9:11119–11125. <https://doi.org/10.18632/oncotarget.24264>.
  40. Hiroshima Y, Zhang Y, Murakami T, Maawy A, Miwa S, Yamamoto M, Yano S, Sato S, Momiyama M, Mori R, Matsuyama R, Chishima T, Tanaka K, et al. Efficacy of tumor-targeting Salmonella typhimurium A1-R in combination with anti-angiogenesis therapy on a pancreatic cancer patient-derived orthotopic xenograft (PDOX) and cell line mouse models. *Oncotarget*. 2014; 5:12346–12357. <https://doi.org/10.18632/oncotarget.2641>.
  41. Fu X, Guadagni F, Hoffman RM. A metastatic nude-mouse model of human pancreatic cancer constructed orthotopically with histologically intact patient specimens. *Proc Natl Acad Sci USA*. 1992; 89:5645–5649.
  42. Hiroshima Y, Maawy A, Zhang Y, Murakami T, Momiyama M, Mori R, Matsuyama R, Katz MH, Fleming JB, Chishima T, Tanaka K, Ichikawa Y, Endo I, et al. Metastatic recurrence in a pancreatic cancer patient derived orthotopic xenograft (PDOX) nude mouse model is inhibited by neoadjuvant chemotherapy in combination with fluorescence-guided surgery with an anti-CA 19–9-conjugated fluorophore. *PLoS One*. 2014; 9:e114310.
  43. Hiroshima Y, Maawy AA, Katz MH, Fleming JB, Bouvet M, Endo I, Hoffman RM. Selective efficacy of zoledronic acid on metastasis in a patient-derived orthotopic xenograft (PDOX) nude-mouse model of human pancreatic cancer. *J Surg Oncol*. 2015; 111:311–315.
  44. Furukawa T, Kubota T, Watanabe M, Kitajima M, Hoffman RM. Orthotopic transplantation of histologically intact clinical specimens of stomach cancer to nude mice: correlation of metastatic sites in mouse and individual patient donors. *Int J Cancer*. 1993; 53:608–612.
  45. Kawaguchi K, Murakami T, Chmielowski B, Igarashi K, Kiyuna T, Unno M, Nelson SD, Russell TA, Dry SM, Li Y, Eilber FC, Hoffman RM. Vemurafenib-resistant BRAF-V600E mutated melanoma is regressed by MEK targeting drug trametinib, but not cobimetinib in a patient-derived orthotopic xenograft (PDOX) mouse model. *Oncotarget*. 2016; 7:71737–71743. <https://doi.org/10.18632/oncotarget.12328>.
  46. Kawaguchi K, Igarashi K, Murakami T, Chmielowski B, Kiyuna T, Zhao M, Zhang Y, Singh A, Unno M, Nelson SD, Russell TA, Dry SM, Li Y, et al. Tumor-targeting Salmonella typhimurium A1-R combined with temozolomide regresses malignant melanoma with a BRAF-V600 mutation in a patient-derived orthotopic xenograft (PDOX) model. *Oncotarget*. 2016; 7:85929–85936. <https://doi.org/10.18632/oncotarget.13231>.
  47. Kawaguchi K, Igarashi K, Murakami T, Zhao M, Zhang Y, Chmielowski B, Kiyuna T, Nelson SD, Russell TA, Dry SM, Li Y, Unno M, Eilber FC, et al. Tumor-targeting Salmonella typhimurium A1-R sensitizes melanoma with a BRAF-V600E mutation to vemurafenib in a patient-derived orthotopic xenograft (PDOX) nude mouse model. *J Cell Biochem*. 2017; 118:2314–2319.
  48. Yamamoto M, Zhao M, Hiroshima Y, Zhang Y, Shurell E, Eilber FC, Bouvet M, Noda M, Hoffman RM. Efficacy of tumor-targeting Salmonella typhimurium A1-R on a melanoma patient-derived orthotopic xenograft (PDOX) nude-mouse model. *PLoS One*. 2016; 11:e0160882.
  49. Hoffman RM. Patient-derived orthotopic xenografts: better mimic of metastasis than subcutaneous xenografts. *Nat Rev Cancer*. 2015; 15:451–452.
  50. Hoffman RM. Development of recombinant methioninase to target the general cancer-specific metabolic defect of methionine dependence: a 40-year odyssey. *Expert Opin Biol Ther*. 2015; 15:21–31.
  51. Mecham JO, Rowitch D, Wallace CD, Stern PH, Hoffman RM. The metabolic defect of methionine dependence occurs frequently in human tumor cell lines. *Biochem Biophys Res Commun*. 1983; 117:429–434.
  52. Yoshioka T, Wada T, Uchida N, Maki H, Yoshida H, Ide N, Kasai H, Hojo K, Shono K, Maekawa R, Yagi S, Hoffman RM, Sugita K. Anticancer efficacy *in vivo* and *in vitro*, synergy with 5-fluorouracil, and safety of recombinant methioninase. *Cancer Research*. 1998; 58:2583–2587.
  53. Tan Y, Sun X, Xu M, Tan XZ, Sasson A, Rashidi B, Han Q, Tan XY, Wang X, An Z, Sun FX, Hoffman RM. Efficacy of recombinant methioninase in combination with cisplatin on human colon tumors in nude mice. *Clinical Cancer Research*. 1999; 5:2157–2163.
  54. Kokkinakis DM, Hoffman RM, Frenkel EP, Wick JB, Han Q, Xu M, Tan Y, Schold SC. Synergy between methionine

- stress and chemotherapy in the treatment of brain tumor xenografts in athymic mice. *Cancer Research*. 2001; 61:4017–4023.
55. Igarashi K, Kawaguchi K, Kiyuna T, Miyake K, Murakami T, Yamamoto N, Hayashi K, Kimura H, Miwa S, Tsuchiya H, Hoffman RM. Effective metabolic targeting of human osteosarcoma cells *in vitro* and in orthotopic nude-mouse models with recombinant methioninase. *Anticancer Res*. 2017; 37:4807–4812.
  56. Yang Z, Wang J, Yoshioka T, Li B, Lu Q, Li S, Sun X, Tan Y, Yagi S, Frenkel EP, Hoffman RM. Pharmacokinetics, methionine depletion, and antigenicity of recombinant methioninase in primates. *Clinical Cancer Research*. 2004; 10:2131–2138.
  57. Yang Z, Wang J, Lu Q, Xu J, Kobayashi Y, Takakura T, Takimoto A, Yoshioka T, Lian C, Chen C, Zhang D, Zhang Y, Li S, et al. PEGylation confers greatly extended half-life and attenuated immunogenicity to recombinant methioninase in primates. *Cancer Research*. 2004; 64:6673–6678.
  58. Tan Y, Zavala Sr J, Xu M, Zavala Jr J, Hoffman RM. Serum methionine depletion without side effects by methioninase in metastatic breast cancer patients. *Anticancer Research*. 1996; 16:3937–3942.
  59. Tan Y, Zavala J Sr, Han Q, Xu M, Sun X, Tan XZ, Tan XY, Magana R, Geller J, Hoffman RM. Recombinant methioninase infusion reduces the biochemical endpoint of serum methionine with minimal toxicity in high-stage cancer patients. *Anticancer Research*. 1997; 17:3857–3860.
  60. Hoffman RM, Erbe RW. High *in vivo* rates of methionine biosynthesis in transformed human and malignant rat cells auxotrophic for methionine. *Proc Natl Acad Sci USA*. 1976; 73:1523–1527.
  61. Stern PH, Mecham JO, Wallace CD, Hoffman RM. Reduced free-methionine in methionine-dependent SV40-transformed human fibroblasts synthesizing apparently normal amounts of methionine. *J Cell Physiol*. 1983; 117:9–14.
  62. Stern PH, Wallace CD, Hoffman RM. Altered methionine metabolism occurs in all members of a set of diverse human tumor cell lines. *J Cell Physiol*. 1984; 119:29–34.
  63. Stern PH, Hoffman RM. Elevated overall rates of transmethylation in cell lines from diverse human tumors. In *Vitro – Rapid Commun in Cell Biology*. 1984; 20:663–670.
  64. Hoffman RM. Altered methionine metabolism, DNA methylation and oncogene expression in carcinogenesis: a review and synthesis. *Biochim Biophys Acta*. 1984; 738:49–87.
  65. Coalson DW, Mecham JO, Stern PH, Hoffman RM. Reduced availability of endogenously synthesized methionine for S-adenosylmethionine formation in methionine dependent cancer cells. *Proc Natl Acad Sci USA*. 1982; 79:4248–4251.
  66. Jeon H, Kim JH, Lee E, Jang YJ, Son JE, Kwon JY, Lim TG, Kim S, Park JH, Kim JE, Lee KW. Methionine deprivation suppresses triple-negative breast cancer metastasis *in vitro* and *in vivo*. *Oncotarget*. 2016; 7:67223–67234. <https://doi.org/10.18632/oncotarget.11615>.
  67. Singhal T, Narayanan TK, Jacobs MP, Bal C, Mantil JC. 11C-methionine PET for grading and prognostication in gliomas: a comparison study with 18F-FDG PET and contrast enhancement on MRI. *J Nucl Med*. 2012; 53:1709–1715.
  68. Blagosklonny MV. Matching targets for selective cancer therapy. *Drug Discov Today*. 2003; 8:1104–7.
  69. Blagosklonny MV. Teratogens as anti-cancer drugs. *Cell Cycle*. 2005; 4:1518–21.
  70. Blagosklonny MV. Treatment with inhibitors of caspases, that are substrates of drug transporters, selectively permits chemotherapy-induced apoptosis in multidrug-resistant cells but protects normal cells. *Leukemia*. 2001; 15:936–41.
  71. Blagosklonny MV. Target for cancer therapy: proliferating cells or stem cells. *Leukemia*. 2006; 20:385–91.
  72. Apontes P, Leontieva OV, Demidenko ZN, Blagosklonny MV. Exploring long-term protection of normal human fibroblasts and epithelial cells from chemotherapy in cell culture. *Oncotarget*. 2011; 2:222–33. <https://doi.org/10.18632/oncotarget.248>.
  73. Blagosklonny MV. Tissue-selective therapy of cancer. *Br J Cancer* 2003; 89:1147–51.
  74. Tan Y, Xu M, Tan X, Wang X, Saikawa Y, Nagahama T, Sun X, Lenz M, Hoffman RM. Overexpression and large-scale production of recombinant L-methionine- $\alpha$ -deaminog- $\gamma$ -mercaptomethane-lyase for novel anticancer therapy. *Prot Exp Purification*. 1997; 9:233–245.